

SYSTEM PERFORMANCE MODELING OF THE LUNAR FLASHLIGHT CUBESAT INSTRUMENT.

Q. Vinckier¹, P. O. Hayne^{1,2}, J.M. Martinez-Camacho¹, C. Paine¹, B. A. Cohen³, U. J. Wehmeier¹, and R. G. Sellar¹,
¹NASA Jet Propulsion Laboratory, California Institute of Technology, Pasadena CA 91109 (vinckier@jpl.nasa.gov),
²University of Colorado, Boulder CO 80303, ³NASA Goddard Space Flight Center, Greenbelt MD 20771.

Summary: Lunar Flashlight (LF) is an innovative CubeSat mission to be launched by NASA's AES (Advanced Exploration Systems) division on the first SLS (Space Launch System) test flight. LF is dedicated to mapping water ice in the permanently shadowed regions of the lunar south pole by measuring surface reflectance at multiple wavelengths. LF will be one of the first CubeSats performing science measurements beyond low Earth orbit – two other CubeSat missions have been selected to make complementary lunar volatile measurements [1,2] – and the first planetary mission to use multi-band active reflectometry from orbit. Here we present the instrument design overview, theory of operation and preliminary performance analysis.

Introduction: Over the last two decades, several missions have revealed strong indications of the presence of water ice on the Moon using a wide range of techniques. Due to limitations of the measurements thus far acquired, interpretations are varied and no consensus has yet been achieved as to the quantity or distribution of lunar H₂O at concentrations sufficient for in-situ resource utilization (ISRU) [3-8]. Lunar Flashlight (LF) is a 6U (measuring approximately 10×20×30 cm) CubeSat dedicated to detecting, quantifying, and mapping water ice in the Permanently-Shadowed Regions (PSRs) (particularly in cold traps, where the temperature is constantly below the 110K sublimation point) and occasionally-sunlit regions to understand the lunar resource potential for future human and robotic exploration of the Moon.

Instrument: The LF instrument is a multi-band reflectometer based on an optical receiver aligned with four lasers, each emitting in a different wavelength in the shortwave infrared (SWIR) spectral region. As illustrated in Figure 1, these wavelengths correspond to peak absorption for water ice (1.495 and 1.99 μm) and nearby continuum (1.064 and 1.850 μm). The 1.064 μm band has been chosen to enable comparison with data acquired by the LOLA (Lunar Orbiter Laser Altimeter) [6]. The lasers fire sequentially in a repeating sequence for 1 ms each, followed by 1 ms with all lasers off. The optical receiver collects and measures a portion of the light reflected from the lunar surface. The measurement with all lasers off quantifies the background, which is the sum of detector dark current, receiver thermal emission incident on the Science detector, and stray solar illumination reflected from the lunar surface towards the instrument. The instrument background is subtracted in

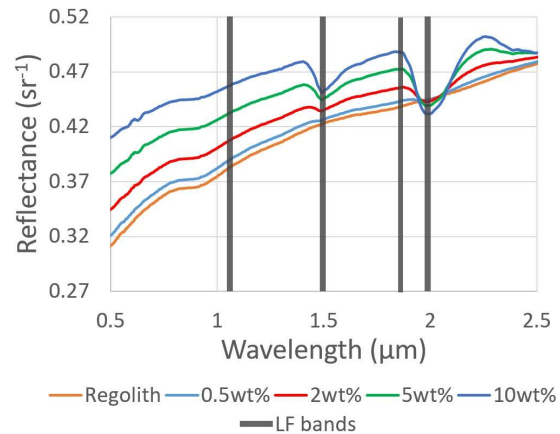


Fig. 1. Reflectance spectrum (bidirectional reflectance) for different water ice contents in lunar regolith at zero phase angle. We calculated these model spectra using Hapke theory [9], with water ice optical constants from [10] and a reflectance spectrum of Apollo 14 lunar highlands sample 14259-85.

post-processing from the measured signals. In order to increase the SNR (Signal-to-Noise Ratio), the measurements are averaged for each of the spectral band over the time in which the laser-illuminated FOV (Field-Of-View) moves a distance on the lunar surface corresponding to the desired mapping resolution of lunar water ice. We derive the reflectance of the lunar surface at each of the four wavelengths and absorption band depths are then analyzed to quantify the weight percent of water ice (wt%) in the illuminated FOV. The science goal is to identify locations where water ice may be present at concentrations $\geq 0.5\text{wt}\%$ (0.5 weight %) on the lunar surface with a mapping resolution of 1-2 km (10 km for the minimum success criteria). During the planned 2-month primary mission, LF will pulse the lasers for several minutes from each of 11 near-rectilinear orbits, at altitudes of 12.6-52.4 km within 10° latitude of the lunar south pole.

The diode lasers, procured from DILAS Inc., will output optical power of 34 W at 1.064 μm , 25 W at 1.495 μm , and 15 W at 1.850 μm and 1.990 μm . > 99.6% of the emitted energy is encircled within a full-angle of 1.15° . The receiver has been designed by Photon Engineering to maximize detection efficiency and uniformity within this FOV. The receiver design has also been optimized to minimize the stray light, i.e. the detection of reflected solar illumination from areas of the lunar surface outside the receiver FOV. The receiver

is based on an a 70×70-mm off-axis bare aluminum paraboloid mirror with a focal length of 70 mm, which collects the incoming light onto a single-pixel, 2 mm diameter, InGaAs detector with a cutoff wavelength of 2.4 μm (at 22°C). The detector temperature is regulated at -65°C during science data acquisition passes in order to maintain a noise equivalent power < 66 fW/Hz^{1/2}. An electronics board amplifies and reads the detector signal in the 0-50 nA current range at 100 kHz, tuned to maximize the SNR for the available data set.

System modeling: We have developed a model that computes the estimated SNR as a function of the spacecraft position based on predicted orbital trajectories of the LF spacecraft. From these SNRs, we then evaluate the fraction of measurements – what we call the “coverage” – for which the SNRs are high enough to discriminate between dry regolith and a given water ice content as a function of the confidence level. The noise contributions that our model takes into account are the following: detector Johnson-Nyquist thermal noise, detector dark current shot noise, detected laser photons shot noise, detector electronics noise, shot noise from instrument thermal emission incident on the detector, and shot noise related to the detected solar background. This last noise contribution is computed using the receiver angular detection efficiency, complex lunar topography at a resolution of 475 m/pixel [11], three-dimensional solar and earthshine illumination of the moon (using the illumination model from [3]), and planned orbital trajectories of the LF spacecraft.

Results and Discussion: The predicted signal due to detected laser photons varies from 9 pA to 240 pA, depending on the wavelength and spacecraft altitude. Our current model indicates that the instrument SNR is driven primarily by the RMS noise of the detector electronics; which in turn is constrained by the available mass and volume. We are currently optimizing the electronics board design to minimize the noise spectral density of this board in order to maximize the overall SNR. For the currently-planned orbital trajectories, our model shows that in order to discriminate water ice at 3σ confidence level with a 0.5wt% resolution and with a mapping resolution of 2 km for 15% of the measurements, the RMS noise spectral density of the reading electronics must be < 1.8×10⁻³ pA/Hz^{1/2}. For a mapping resolution of 10 km, the instrument can discriminate water ice with 0.5wt% resolution at 3σ confidence level for 15% (respectively 40%) of the measurements with electronics RMS noise spectral density of 1.3×10⁻¹ pA/Hz^{1/2} (respectively 9×10⁻² pA/Hz^{1/2}). Fig. 2 shows the instrument SNRs and coverage corresponding to this RMS noise spectral density of 1.3×10⁻¹ pA/Hz^{1/2}. The predicted Science data paths on the lunar South Pole are illustrated in Fig. 3. The noise related to the lasers’ optical power

monitoring system still has to be evaluated and included in our model, as well as the instrument calibration uncertainty.

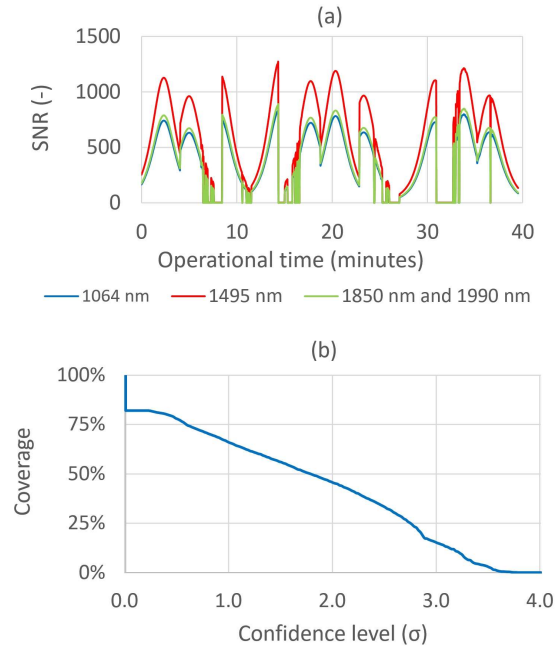


Fig. 2. (a) LF instrument SNRs VS operational time. (b) LF measurements coverage as a function of the confidence level. Mapping resolution: 10 km, water ice discrimination level: 0.5wt%, reading electronics RMS noise spectral density: 1.3×10⁻¹ pA/Hz^{1/2}.

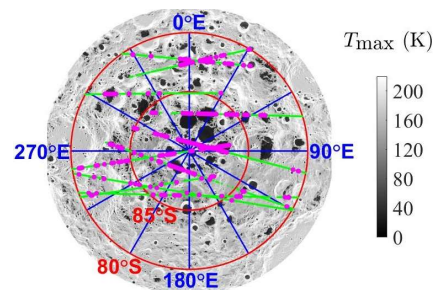


Fig. 3. LF spacecraft Science data paths on the lunar South Pole. The gray scale shows the maximum temperature; the green and pink segments are the Science paths with the pink dots indicating the PSRs.

References: [1] Clark, P. E., et al. (2016) *DPS Meeting*, 48, id.223.03. [2] Hardgrove, C., et al. (2015) *LEAG Meeting*, Abstract #2035. [3] Paige, D. A., et al. (2010) *Science*, 330, 479-482. [4] Mitrofanov, I. G., et al. (2010) *Science*, 330, 483-486. [5] Gladstone, G. R., et al. (2012) *JGR*, 117, E00H04. [6] Zuber, M. T., et al. (2012) *Nature*, 486, 378-381. [7] Hayne, P. O., et al. (2015) *Icarus*, 255, 58-59. [8] McCord, T. B., et al. (2011) *JGR*, 116. [9] Hapke, B. (1981) *JGR*, 86(B4), 3039-3054. [10] Warren, S. G., & Brandt, R. E. (2008) *JGR*, 113(D14). [11] Smith, D. E. et al. (2010) *GRL*, 37, L18204.